

Aberystwyth University

Bolla Bollana boulder beds

Le Heron, Daniel P.; Busfield, Marie E.; Collins, Alan S.

Published in:
Sedimentology

DOI:
[10.1111/sed.12082](https://doi.org/10.1111/sed.12082)

Publication date:
2014

Citation for published version (APA):

Le Heron, D. P., Busfield, M. E., & Collins, A. S. (2014). Bolla Bollana boulder beds: A Neoproterozoic trough mouth fan in South Australia? *Sedimentology*, 61(4), 978-995. <https://doi.org/10.1111/sed.12082>

General rights

Copyright and moral rights for the publications made accessible in the Aberystwyth Research Portal (the Institutional Repository) are retained by the authors and/or other copyright owners and it is a condition of accessing publications that users recognise and abide by the legal requirements associated with these rights.

- Users may download and print one copy of any publication from the Aberystwyth Research Portal for the purpose of private study or research.
- You may not further distribute the material or use it for any profit-making activity or commercial gain
- You may freely distribute the URL identifying the publication in the Aberystwyth Research Portal

Take down policy

If you believe that this document breaches copyright please contact us providing details, and we will remove access to the work immediately and investigate your claim.

tel: +44 1970 62 2400
email: is@aber.ac.uk



Bolla Bollana boulder beds: a Neoproterozoic trough mouth fan in South Australia

Journal:	<i>Sedimentology</i>
Manuscript ID:	SED-2013-OM-055.R1
Manuscript Type:	Original Manuscript
Date Submitted by the Author:	23-Jul-2013
Complete List of Authors:	Le Heron, Daniel; Royal Holloway, University of London, Earth Sciences Busfield, Marie; Royal Holloway, Earth Sciences Collins, Alan
Keywords:	trough mouth fan, Flinders Ranges, Sturtian, Neoproterozoic, Glaciation, snowball Earth, ice stream

Bolla Bollana boulder beds: a Neoproterozoic trough mouth fan in South Australia?

DANIEL P. LE HERON^{*}, MARIE E. BUSFIELD^{*}, ALAN S. COLLINS[†].

^{*}*Department of Earth Sciences, Queen's Building, Royal Holloway University of London, Egham, TW200EX, United Kingdom*

[†]*TRAX, School of Earth and Environmental Sciences, University of Adelaide, SA 5005, Australia*

Abstract

The Bolla Bollana Formation is an exceptionally thick (~1500 m), rift-related sedimentary succession cropping out in the northern Flinders Ranges, South Australia, which was deposited during the Sturtian (mid Cryogenian) glaciation. Lithofacies analysis reveals three distinct facies associations which chart changing depositional styles on an ice-sourced subaqueous fan system. The diamictite facies association is dominant, and comprises both massive and stratified varieties with a range of clast compositions and textures, arranged into thick beds (1- 20 m), representing stacked, ice-proximal glaciogenic debris flow (GDF) deposits. A channel belt facies association, most commonly consisting of normally-graded conglomerates and sandstones, displays scour and fill structure of ~10 m width and 1-3 m depth: these strata are interpreted as channelised turbidites. Rare mud-filled channels in this facies association bear glacially striated limestones. Finally, a sheet heterolithics facies association contains a range of conglomerates through sandstones to silty shales arranged into clear, normally graded cycles from the lamina to bed scale. These record a variety of non-channelised turbidites, probably occupying distal and/or interchannel locations on the subaqueous fan. Coarsening and thickening-up cycles, capped by dolomicrites or mudstones, are indicative of lobe build out and abandonment, potentially as a result of ice lobe advance and stagnation. Dropstones, recognised by downwarped and punctured laminae beneath pebbles to boulders in shale, or in delicate climbing ripple cross-laminated siltstones, are clearly indicative of ice rafting. The co-occurrence of ice-rafted debris and striated limestones strongly support a glaciogenic sediment source for the diamictites. Comparison to Pleistocene analogues enables an interpretation as a trough mouth fan, most probably deposited leeward of a palaeo-ice stream. Beyond emphasising the highly dynamic nature of Sturtian ice sheets, these interpretations testify to the oldest trough-mouth fan recorded to date.

Keywords: Sturtian; Neoproterozoic; Glaciation; snowball Earth; trough mouth fan; ice stream; Flinders Ranges

1
2
3 50
4 51
5 52 **INTRODUCTION**

6 53 The northern Flinders Ranges of South Australia exposes an extremely thick
7
8
9 54 succession of diamictites that were deposited during the Sturt glaciation (Young and
10
11 55 Gostin, 1991; Preiss et al., 2011) at ~715 Ma (Macdonald *et al.*, 2010). In Arkaroola
12
13 56 (**Fig. 1**), these deposits were first described by Mawson (1941, 1949), and interpreted
14
15 57 as terrestrial glacial deposits. By contrast, glaciomarine interpretations were offered
16
17 58 by Young and Gostin (1991) by the recognition of dropstone fabrics. The deposits are
18
19 59 highly contentious and significant to debates focussed on the intensity and extent of
20
21 60 Cryogenian glaciations (e.g. Fairchild and Kennedy, 2007; Etienne et al., 2007; Allen
22
23 61 and Etienne, 2008), particularly as South Australia can be regarded as a type area for
24
25 62 the “Sturtian” pan-glacial event (Hoffman and Schrag, 2002).
26
27
28
29 63

30
31 64 For some, scepticism surrounds the interpretation of many Cryogenian
32
33 65 diamictite-bearing successions, such as those in the Flinders Ranges. A mechanism of
34
35 66 diachronous rift shoulder glaciation, during the fragmentation of Rodinia, was
36
37 67 proposed by Eyles and Januszczak (2004). In that model, debris flows were fluxed
38
39 68 into rift basins. In Namibia, for example, it was proposed that some diamictites were
40
41 69 deposited by non-glacially influenced gravity flow deposits (Eyles & Januszczak,
42
43 70 2007), amplifying Schermerhorn’s earlier non-glacial interpretations (Schermerhorn
44
45 71 and Stanton, 1963; Schermerhorn, 1974). Such studies have hence stimulated
46
47 72 questions about the clarity of the glacial signature in Neoproterozoic sedimentary
48
49 73 successions. Recent examples worldwide, however, highlight the diverse range of
50
51 74 reliable glaciogenic proxies preserved, despite tectonically active basin configurations
52
53 75 (e.g. Arnaud, 2012; Busfield and Le Heron, in press; Le Heron et al., 2011, 2012;
54
55 76 Uhlein et al. 2011). These studies provide substantive evidence for glacial processes
56
57
58
59
60

1
2
3 77 during the Neoproterozoic, irrespective of the scale of interpreted ice sheets (cf. Allen
4
5 78 and Etienne, 2008).
6

7 79
8

9
10 80 In this paper, a detailed facies analysis of the Bolla Bollana Formation in the
11
12 81 northern Flinders Ranges (**Fig. 1, 2**) is undertaken, presenting data from three
13
14 82 outstanding exposures. The succession is part of a classic diamictite succession which
15
16 83 has not been subjected to detailed investigation for over 20 years. The data were
17
18 84 collected as part of a six week field campaign in August 2012.
19

20
21 85

22 86

23 87 **STUDY AREA AND STRATIGRAPHY**

24 88 In the Arkaroola district of the northern Flinders Ranges, the lowermost of two
25
26 89 Neoproterozoic diamictite-bearing intervals is exposed. These rocks belong to the
27
28 90 Yudnamutana Subgroup (**Fig. 3**). A threefold subdivision of this subgroup is
29
30 91 recognised: the Fitton Formation occurs at the base, the Bolla Bollana Formation in
31
32 92 the middle, and the Lyndhurst Formation is the uppermost unit (**Fig. 3**). The Bolla
33
34 93 Bollana Formation was first examined in the Arkaroola district by Mawson (1941,
35
36 94 1949). This pioneering work offered a terrestrial glacial origin for the diamictites. The
37
38 95 formation itself was defined by Coats (in Thomson et al., 1964) as a subgreywacke
39
40 96 tillite of massive character with intercalated quartzite and siltstone. Young and Gostin
41
42 97 (1988, 1989, 1990, 1991) studied the Sturtian succession within the North Flinders
43
44 98 Basin (NFB), a sub-basin within the Adelaide Fold Belt that Preiss (1987, 1998, 2000)
45
46 99 argued was likely disconnected from depocentres in the central and southern Flinders
47
48
49
50 100 Ranges. Each paper presented a series of sedimentary logs, and facies descriptions,
51
52 101 recognising a comparable stratigraphic subdivision across the area. The dramatic
53
54 102 increase in knowledge of sedimentary processes at tidewater ice margins since the
55
56 103 time of Mawson motivated Young and Gostin (1989, 1991) to re-interpret the Bolla
57
58
59
60

1
2
3 104 Bollana Formation as glaciomarine. Regional mapping (Coats, 1973) demonstrates
4
5 105 that the Bolla Bollana Formation is extensive in the eastern part of the Copley Sheet,
6
7 106 and is particularly well exposed to the east and south of Arkaroola (**Fig. 1**).
8
9
10 107 Summarising the regional stratigraphy, Young and Gostin (1991) published a map
11
12 108 showing how sediment dispersal, surmised from a variety of palaeocurrent indicators,
13
14 109 testifies to the interplay of extensional tectonics, forming graben-like minibasins, and
15
16 110 palaeohighs (**Fig. 2**).
17
18
19 111

20
21 112 The Bolla Bollana Formation trends toward massive in character in the south
22
23 113 of the NFB, becoming stratified in the north. To explain this, Young and Gostin
24
25 114 (1988) suggested that ice-rafted debris (IRD) deposition was predominant in the
26
27 115 south, with reworking processes more important northward. No unequivocal glacially
28
29 116 striated surfaces are reported in Cryogenian successions of Australia, with the
30
31 117 exception of those in Western Australia (Corkeron, 2007). However, the “cast of
32
33 118 striations” is reported to occur “on the underside of basal Sturt silty mudstones near
34
35 119 Merinjina Well” (Young and Gostin, 1991). These were interpreted as tectonic by
36
37 120 Daily *et al.* (1973), and glaciogenic by others (Preiss, 1987; Young and Gostin, 1991;
38
39 121 Preiss *et al.*, 2011).
40
41
42
43
44

45 123 In our present paper, detailed facies descriptions and interpretations are
46
47 124 provided from three new sections at Stubb’s Waterhole, Tillite Gorge, and Weetootla
48
49 125 Gorge. None of these sections were investigated by Young and Gostin (1991), yet
50
51 126 they yield exceptionally high quality exposure. The sections are ideally situated in a
52
53 127 region subject to only low grade metamorphism during the Early Palaeozoic
54
55 128 Delamerian Orogeny (Preiss, 1987), whereas mid-amphibolite facies affect correlative
56
57
58
59
60

1
2
3 129 sediments in the Adelaide region. Our objectives are (1) to highlight a clear
4
5 130 glaciogenic source for the Bolla Bollana Formation, (2) to reject a rift-only origin for
6
7 131 diamictites, and (3) to present a new depositional model for the sequence as a trough-
8
9 132 mouth fan succession.
10

11
12 133

134 **FACIES ANALYSIS**

135 The thickness of the Yudnamutana Subgroup in the North Flinders Basin is estimated
16
17 136 to reach 6000 m in the Yudnamutana Trough (Young and Gostin, 1991),
18
19 137 approximately 30 km NW of the study area. Herein, we focus on exceptionally well-
20
21 138 preserved, high quality sections rather than attempting a complete stratigraphic
22
23 139 traverse. Each of the three facies associations described and interpreted below occur
24
25 140 in multiple locations in the Arkaroola district. We recognise a diamictite facies
26
27 141 association, a channel belt facies association, and a sheet heterolithics facies
28
29 142 association. Below, data from three detailed logged sections are presented (**Fig. 4**).
30
31
32
33

34 143

35 36 144 **Diamictite facies association**

37
38 145

39 40 146 *Description*

41
42
43 147 This facies association is highly heterogeneous and in terms of volume dominates the
44
45 148 Bolla Bollana Formation (**Fig. 5 A**). Uninterrupted accumulations >90 m thick are
46
47 149 common (e.g. Tillite Gorge: **Fig. 4 B**; **Fig. 5 A**). Diamictites are sandy throughout,
48
49 150 including both clast-poor and clast-rich varieties (*sensu* Moncrieff, 1989), with pebble
50
51 151 to predominantly boulder sized clasts. Bed thickness varies considerably between 1-
52
53 152 15 m (thus reaching megabed dimensions *sensu* Marjanac, 1996) (**Fig. 5 B**). With
54
55
56
57
58
59
60

1
2
3 153 some exceptions, most bed contacts are parallel to one another with minimal evidence
4
5 154 for erosive contacts.
6

7 155

8
9
10 156 Both massive and well stratified diamictites occur as end-members of a
11
12 157 continuum; most beds exhibit at least some diffuse stratification. In some cases,
13
14 158 pronounced variations in clast content (20-60%) occur in successive beds (e.g. **Fig. 4**
15
16 159 **A**, 15-25 m; **Fig. 5 C**). In thick beds, upward transitions from stratified through
17
18 160 massive facies occur, accompanied by an increase in clast size and content (**Fig. 4 B**,
19
20 161 43-73 m). In stratified clast-poor diamictites, isolated clasts of pebble to boulder size
21
22 162 downwarp and pierce underlying laminations; overlying laminae are unaffected (**Fig.**
23
24 163 **5 D**). Sand lenses, or lens-shaped clast-free zones in the diamictite, occur both at the
25
26 164 bottom and top of some beds. Throughout the facies association, clasts are typically
27
28 165 equant, and sub-rounded to sub-angular. The base of the thickest observed bed in the
29
30 166 Tillite Gorge section (**Fig. 4 B**, 43 m) shows a highly undulose contact(**Fig. 5 E**).
31
32 167 Clasts with polished surfaces and crosscutting striations locally occur (**Fig. 5 F**).
33

34 168

35 169 *Interpretation*

36
37
38 170 The diamictite facies association is interpreted largely as a suite of glaciogenic debris
39
40 171 flows (GDFs) deposited in a subaqueous setting. The organisation of the diamictites
41
42 172 into clearly defined beds indicates repeated emplacement of flows. The typical
43
44 173 absence of erosive contacts is attributed to hydroplaning at the head of the flow,
45
46 174 thereby lubricating the base of the flow and protecting the underlying bed from
47
48 175 cannibalisation (e.g. Laberg and Vorren, 2000). The upsection increase in clast
49
50 176 abundance and size is consistent with kinetic sieving within the flow, to generate
51
52 177 inverse grading (Talling *et al.*, 2012). The downwarping of laminae beneath pebbles
53
54
55
56
57
58
59
60

1
2
3 178 in the stratified clast-poor diamictites (**Fig. 5 D**) are interpreted as impact structures
4
5 179 produced by falling dropstones. Whilst clasts sinking into water saturated sediment
6
7 180 can produce dropstone-like texture in a debris flow, such clasts typically behave
8
9 181 similarly to tectonic augen, with concomitant shearing of adjacent laminae as the flow
10
11 182 evolves (Hart and Roberts, 1994). Thus, in addition to downslope mass flow, evidence
12
13 183 for subaqueous sedimentation and ice-rafted debris accumulation is preserved. Given
14
15 184 the compositional similarity of strata both below and above the undulose bed contacts,
16
17 185 (**Fig. 5 E**) it is likely that this feature developed through differential compaction rather
18
19
20 186 than through erosion. The presence of clasts with crosscutting striations (**Fig. 5 F**)
21
22 187 strongly supports glacial derivation. Specifically, the crosscutting striations indicate
23
24
25 188 rotation of the clasts, either in basal ice, at the ice-bed interface, or within the
26
27 189 deforming bed beneath an ice mass (Benn and Evans, 2010, p. 361). The exceptional
28
29 190 preservation of striations supports incorporation into the GDFs via ice-rafting, thereby
30
31 191 protecting clast surfaces from the erosion processes anticipated during downslope re-
32
33 192 mobilisation.
34
35

36 193

37
38 194 **Channel belt facies association**39
40 19541
42 196 *Description*

43
44 197 A variety of scour and fill structures, measuring 5-14 m wide, and 2-3.5 m depth, are
45
46 198 a key feature of this facies association (**Fig. 4 B**, 95-113 m; **Fig. 6 A, B**). The scours
47
48 199 crosscut, with multiple generations apparent over a few metres (**Fig. 6 A, B**).

50 200 Lithologies include pebble to granule conglomerates, sandstones and siltstones,
51
52 201 together with subordinate sandy diamictites. Some of the scours are mud-filled and re-
53
54 202 incised by an overlying channel (**Fig. 6 C**). The base of most beds is irregular (**Fig. 6**

1
2
3 203 D). Normally-graded bedding is typical, with transitions from granule conglomerate
4
5 204 through planar-bedded sandstone well expressed in Tillite Gorge as R1 through S3
6
7 205 turbidite divisions of Lowe (1982) (e.g. **Fig. 4 B**, 99-103 m; **Fig. 7A**). Soft-sediment
8
9 206 deformation structures in sandstone include recumbent folds (**Fig. 7 B**), curvilinear
10
11 207 grooves on the upper surfaces of sandstone beds (**Fig. 7 C**) and flame structures. This
12
13 208 suite of deformation structures is concentrated at a discrete stratigraphic interval
14
15
16 209 (“shear zone” at 25 m, log B, Fig. 4). Sandy diamictites form sheet-like beds of 0.3-1
17
18 210 m, and contain sub-rounded to rounded clasts with striated faces (**Fig. 7 D**).
19
20
21 211 Siltstones occur both within channel structures, and as sheet-like lithosomes traceable
22
23 212 for several tens of metres. In both cases, siltstones are poorly stratified, yet bear rare
24
25 213 clasts of pebble to boulder size; these pierce and downwarp underlying laminations,
26
27 214 with overlying laminations unaffected (**Fig. 7 E, F**).
28
29
30
31

32 *Interpretation*

33
34 217 The scour and fill structures are interpreted as channels cut by turbidity currents and
35
36 218 filled with turbidites. The coarse calibre of some of the channel fills, and the
37
38 219 characteristic R1 through S3 turbidite motif (Lowe, 1982), implies a relatively
39
40 220 proximal location on the fan (Reading and Richards, 1994). The particularly coarse-
41
42 221 calibre (gravelly) material at the base of some channels is suggestive of a lag deposit
43
44 222 (Alpak et al., 2013). By comparison, the finer-grained channel fills are interpreted to
45
46 223 record lower energy deposition in either a slightly more distal location on the fan or
47
48 224 alternatively a finer-grained sediment source. Specifically, silt-plugged channels may
49
50 225 suggest that the channels are filled by low density turbidites (Talling et al., 2012).
51
52 226 These deposits represent off-axis / channel margin facies (Camacho *et al.*, 2002) or
53
54 227 coarse-grained sediment bypass (Talling et al., 2012), and probably record deposition
55
56
57
58
59
60

1
2
3 228 of these turbidites more distal to the sediment source than their coarser-grained
4
5 229 counterparts.

6
7 230

8
9 231 The suite of soft-sediment deformation structures is compatible with rapid
10
11 232 subaqueous deposition: recumbent folds can be indicative of gravitational instability
12
13 233 and downslope slumping (Maltman, 1994), whereas flame structures are probably
14
15 234 examples of Rayleigh-Taylor instabilities generated at a grain-size / bed interface
16
17 235 (Allen, 1984; Collinson and Thompson, 1987). Numerical modelling of flame
18
19 236 structures indicates that their genesis is promoted when relatively low viscosity,
20
21 237 Newtonian fluids (the sand layer) rest on underlying clays (Harrison and Maltman,
22
23 238 2003). These conditions may be satisfied by rapid sedimentation or liquefaction. The
24
25 239 curvilinear grooves on the upper surface of beds are interpreted as intra-bed slip
26
27 240 planes, akin to hydroplastic slickensides (Petit and Laville, 1987) produced by the
28
29 241 shearing of soft sediment in response to downslope movement. Shanmugam *et al.*
30
31 242 (1995) described similar features from the Cretaceous and Palaeogene of the North
32
33 243 Sea. A later tectonic origin can be dismissed on account of their local occurrence,
34
35 244 curvilinear geometry, absence of asperities, and lack of mineralisation (c.f. Petit and
36
37 245 Laville, 1987).

38
39 246

40
41 247 The presence of “impact structures” (curvature, deflection and puncturing of
42
43 248 underlying laminations: Bennett *et al.*, 1996) beneath limestones clearly points to ice-
44
45 249 rafted debris (IRD) (e.g. Eyles *et al.*, 2007). Moreover, the presence of polished and
46
47 250 striated clast surfaces also indicates a clear glacial derivation. Despite the absence of
48
49 251 impact structures in the sheet-like siltstones, the presence of limestones may likewise
50
51 252 indicate rafting from icebergs, or alternatively sub-ice shelf deposition (Benn and
52
53
54
55
56
57
58
59
60

1
2
3 253 Evans, 2010). By analogy to comparable facies in the diamictite facies association,
4
5 254 the diamictites in the channel belt facies association are also interpreted as the product
6
7 255 of glaciogenic debris flows.
8

9
10 256

11 257 **Sheet heterolithic facies association**

12
13
14 258

15 259 *Description*

16
17
18 260 These deposits include a heterogeneous collection of lithologies ranging from granule
19
20 261 conglomerates and diamictites, sandstones, siltstones, shales and dolostones. At
21
22 262 outcrop, these lithologies are well differentiated, forming tabular beds that can be
23
24 263 traced for tens to hundreds of metres along strike. Decimetre to metre-scale fining
25
26 264 upward cycles is typical, with well-expressed examples in Weetootla Gorge (**Fig. 4 C**,
27
28 265 23-75 m; **Fig. 8 A**). Fining upward cycles commence with sharp-based and locally
29
30 266 scoured surfaces, overlain by granule-lags or massive sandstones (**Fig. 8 B**),
31
32 267 becoming parallel laminated upsection. Supercritical climbing ripple cross-laminated
33
34 268 sandstones and siltstones (**Fig. 8 C**) are typical in the upper part of many fining
35
36 269 upward cycles (e.g. 56 m, 68 m, 85 m, 100 m at Weetootla Gorge: **Fig. 4 C**). The
37
38 270 crests of the ripple-cross laminae show an aggradational to weakly progradational
39
40 271 character (**Fig. 8 C**). Rarely, the fining upward intervals are interrupted by clast-poor,
41
42 272 sandy diamictites which do not exceed 1 m in thickness (**Fig. 8 D**). Siltstone and shale
43
44 273 occur at the top of the fining upward cycles (**Fig. 8 E**). Lonestones with impact
45
46 274 structures occur in most facies, including the cross-laminated sandstone (e.g. 102 m,
47
48 275 Tillite Gorge: **Fig. 4 B**; **Fig. 8 B**, arrowed clast) and in shale beds (**Fig. 8 E**). The
49
50 276 metre-scale fining upward cycles are themselves organised into multi-metre thick
51
52 277 coarsening and fining upward motifs. At three intervals (25 m, 37 m, 66.5 m at
53
54
55
56
57
58
59
60

1
2
3 278 Weetootla Gorge: **Fig. 4 C**) we observed buff coloured, delicately parallel laminated,
4
5 279 mud-grade dolostones (**Fig. 8 F**).

6
7 280

8
9
10 281 *Interpretation*

11 282 This facies association is interpreted to represent deposition in an inter-channel part of
12
13 283 a subaqueous fan system, where the well-expressed, metre-scale fining upward cycles
14
15 284 are interpreted to record repeated emplacement of turbidity flows. A basal scour and
16
17 285 lag, succeeded by a massive then parallel laminated sandstone interval, succeeded by
18
19 286 climbing ripple cross-lamination, is a motif common to all models of turbidite genesis
20
21 287 (c.f. Bouma, 1962; Lowe, 1982; Mutti, 1996; Talling *et al.*, 2012). Whilst the tabular
22
23 288 geometry of the cycles is compatible with deposition as high-density turbidites (i.e.
24
25 289 divisions T_A, T_{B-2} and T_{B-3} in the modified Bouma nomenclature: Talling *et al.*, 2012)

26
27 290 The occurrence of lonestones with impact structures, interpreted as dropstones, in
28
29 291 ripple cross-laminated siltstones is strong evidence for glacial influence. The
30
31 292 supercritical styles of ripple cross-lamination testify to high rates of sediment
32
33 293 delivery, and tractive velocities of $<0.6 \text{ m s}^{-1} \text{ m}$ (e.g. Bridge and Demicco, 2008). The
34
35 294 occurrence of large clasts within these facies is at odds with the low velocities
36
37 295 required for the formation of ripple cross-lamination, which are thus interpreted as
38
39 296 ice-rafted debris. Furthermore, turbidity flows typically demonstrate low yield
40
41 297 strength and cannot support clasts through buoyancy within the flow (Shanmugam,
42
43 298 2002). Although Lowe (1982) suggested that sand-dominated traction carpets in dense
44
45 299 sandy turbidites were capable of periodically bouncing clasts as suspension load,
46
47 300 these inferred processes have not been observed in turbidity currents (Talling *et al.*,
48
49 301 2012). The co-occurrence of thin sandy diamictites, interpreted as the dilute distal
50
51
52
53
54
55
56
57
58
59
60

1
2
3 302 fronts of glaciogenic debris flows, strengthens the interpretation of a glacial influence
4
5 303 on sedimentation.
6

7 304

8
9 305 The organisation of the Bouma cycles into both coarsening and fining upward
10
11 306 motifs at the multi-metre scale is respectively suggested to record the buildout and
12
13 307 abandonment of subaqueous fan lobes, in a similar manner to other glacially sourced
14
15 308 subaqueous fan systems (Le Heron et al., 2008). The delicately laminated dolostones
16
17 309 at the top of some fining-upward cycles remains cryptic. They do not occur in finer-
18
19 310 grained, turbidite-dominated systems of the central Flinders Ranges (e.g. Busfield and
20
21 311 Le Heron, in review; Le Heron et al., 2011), which likely indicates that the dolostones
22
23 312 are of local significance. They are presently suggested to record chemical or
24
25 313 biological precipitation during or following lobe abandonment, although the precise
26
27 314 mechanisms of precipitation requires further study. Their lonestone-free textures merit
28
29 315 one further consideration, however. If subaqueous sedimentation rates of IRD were
30
31 316 similar everywhere on the fan system at a given time, comparable deposits should
32
33 317 form simulatenously. Given the absence of lonestones in the dolostones, intervals of
34
35 318 IRD-free conditions might be proposed, thus suggesting that these might be associated
36
37 319 with lower rates of deposition and therefore no floating ice.
38
39
40
41
42
43
44
45
46

47 320

48 321

49 322 **STACKING PATTERNS**

50 323 The vertical stacking motif of facies associations is an important consideration in a
51
52 324 glacially-sourced sedimentary system and may allow the dynamics of former ice
53
54 325 sheets to be elucidated. At Stubb's Waterhole, the diamictite facies association
55
56 326 predominates but those strata are intercalated with ~5 m thick developments of the
57
58
59
60

1
2
3 327 sheet heterolithic facies association. A considerably thicker example of that facies
4
5 328 association is found interbedded with the diamictite facies association at Weetootla
6
7 329 Gorge (23- 75 m: **Fig. 4 C**). Given the differences in thickness at both localities, it is
8
9 330 proposed that the Stubb's Waterhole occurrence may represent the margins of a
10
11 331 turbidite lobe system (e.g. Pr elat et al., 2010), whereas the Weetootla Gorge examples
12
13 332 are more compatible with the core of a turbidite lobe system. Note, however, that our
14
15 333 data do not represent a complete traverse through the formation in either case.
16
17
18 334 Interstratification of the diamictite facies association and the channel belt facies
19
20 335 association, at the tens of metres scale at Tillite Gorge testifies to the likely
21
22 336 synchronous co-development of turbidite channel belts and GDF deposits. This
23
24 337 implies that each sub-environment, recognised in the form of the three facies
25
26 338 associations, co-existed during deposition of the Bolla Bollana Formation.
27
28
29
30 339

31
32 In the Arkaroola area, the Bolla Bollana Formation maps as a continuous
33
34 341 stratigraphic unit around the north-eastern extremity of the Gammon Ranges. Preiss *et*
35
36 342 *al.* (1993, 1998, 2000, 2011), interpret the North Flinders Basin as a region that
37
38 343 experienced extension synchronous with glaciation by Sturtian ice sheets. Progressive
39
40 344 thickness increases to the north are explained by the development of an echelon half
41
42 345 graben (Preiss et al., 2011). Crustal extension, during the fragmentation of Rodinia,
43
44 346 which accounted for the generation of substantive accommodation space, was also
45
46 347 considered to be important by Young and Gostin (1988, 1989, 1990, 1991). However,
47
48 348 the location of many of these faults remains unclear: the 1:250,000 sheet (Copley:
49
50 349 Coats, 1973) reveals no faults specifically causing abrupt thickness changes in the
51
52 350 Bolla Bollana Formation.
53
54
55
56
57
58
59
60

1
2
3 352 We argue that the substantial thickness and sedimentary architecture of the
4
5 353 Bolla Bollana Formation can be explained by ice sheet dynamics alone. The
6
7 354 diamictite facies association records glaciogenic debris flows (GDFs) with secondary
8
9 355 ice-rafting in the proximal part of a subaqueous basin (**Fig. 9**). The presence of
10
11 356 faceted, polished and striated clasts in the Bolla Bollana Formation strongly implies
12
13 357 direct glacial derivation. This is because cannibalised or reworked (second
14
15 358 generation) debris flows tend to erode and smooth clast surfaces (Le Heron *et al.*,
16
17 359 2013). The glaciogenic debris flows likely became diluted basinward, developing into
18
19 360 turbulent underflows, which built up a series of lobes and channel belts (i.e. channel
20
21 361 belt facies association) on a large subaqueous fan (**Fig. 9**). The sheet heterolithics
22
23 362 facies association represents lobe deposits (e.g. Pr lat *et al.*, 2010) in the inter-channel
24
25 363 part of a subaqueous fan system. These lobes were influenced by local ice rafting as a
26
27 364 secondary sediment source (**Fig. 9**). Abandonment of the lobes locally resulted in
28
29 365 some highly unusual laminated dolostone deposits. These superficially resemble “cap
30
31 366 dolostone” deposits (e.g. Rose and Maloof, 2010). As noted earlier, given their
32
33 367 probable stratigraphic context as lobe abandonment facies it is unlikely that they have
34
35 368 any wider significance. The lack of evidence for IRD in these specific facies- a
36
37 369 texture which might be expected to appear more prominently once sediment supply is
38
39 370 arrested- is also puzzling.
40
41
42
43
44
45
46
47
48

371

372

373 **A NEOPROTEROZOIC TROUGH-MOUTH FAN?**

374 It is suggested that the Bolla Bollana Formation is a trough mouth fan (TMF) (**Fig. 9**)
375 deposited seaward of a comparatively small palaeo-ice stream. This interpretation is
376 fully consistent with 1) clear evidence for glacial processes in every facies association

1
2
3 377 of the Bolla Bollana Formation, 2) the substantial thickness of the succession which
4
5 378 compares closely to stacked mass flow deposits of the Bear Island Fan (Taylor *et al.*,
6
7 379 2002; Ó Cofaigh *et al.*, 2003), and 3) the stratigraphic motif and nature of the facies
8
9 380 associations preserved.

10
11 381

12
13
14 382 Evidence for glaciation throughout the Bolla Bollana Formation is pervasive
15
16 383 and includes dropstone textures (in turbidites, as well as hemipelagic muds), together
17
18 384 with faceted, polished and striated clasts throughout the succession. Boreholes sunk
19
20 385 in the Uummannaq Fan (western Greenland) illustrate 300 m thick successions of
21
22 386 diamicton that are sharply overlain by mud (Ó Cofaigh *et al.*, 2012). These are closely
23
24 387 comparable to stacked examples of the diamictite facies association in Tillite Gorge.
25
26 388 Intercalated debrites, turbidites, and ice-rafted debris commonly occur together in
27
28 389 depositional models of Pleistocene TMFs (Ó Cofaigh *et al.*, 2012).

29
30
31
32 390

33
34 391 In both the northern and southern hemispheres, trough mouth fans (TMFs)
35
36 392 were deposited during Pleistocene glaciations and consist of thick accumulations of
37
38 393 glaciogenic detritus (Escutia *et al.*, 2000; Taylor *et al.*, 2002). In this process, fast-
39
40 394 flowing ice streams excavate the subglacial substrate and deposit diamictite at the ice
41
42 395 front, perched landward of the slope break. In Pleistocene examples, rapid
43
44 396 sedimentation of water saturated tills led to unstable slope angles and hence
45
46 397 intermittent failure (Dowdeswell *et al.*, 2002). This in turn led to the generation of
47
48 398 GDFs derived from collapsing tills (Taylor *et al.*, 2002). In the southern hemisphere,
49
50 399 the Wilkes Land continental margin was fed by stacked GDFs, which evolved
51
52 400 downslope into turbidites, building up a multi-kilometre thick pile of channelized
53
54 401 proglacial detritus (Escutia *et al.*, 2000).

1
2
3 402
4
5 403 Regional mapping (Coats, 1973) shows that the Bolla Bollana Formation
6
7 404 crops out over at least 1800 km². Assuming a conservative thickness of 1 km in the
8
9 405 Arkaroola district, the Bolla Bollana Formation represents approximately 1800 km³ of
10
11 406 glaciogenic sediment: impressive, yet substantially less volumetric than the modern
12
13 407 Bear Island Fan (ca. 340,000 km³) (Dowdeswell *et al.*, 2002 and refs therein). Part of
14
15 408 the reason for this comparatively small volume may lie in the partitioning of the basin
16
17 409 by syn-depositional faults (Preiss *et al.*, 2011). From both stratigraphic and facies
18
19 410 perspectives, there is good reason to view the North Flinders Basin as a sub-basin
20
21 411 disconnected from the central Flinders Ranges further to the south (Preiss *et al.*,
22
23 412 2011). Differences between Pleistocene TMF models and our interpretation (**Fig. 9**)
24
25 413 include the absence of bioturbation and a lower volume of mud in the Bolla Bollana
26
27 414 TMF deposit (c.f. Ó Cofaigh *et al.*, 2002; 2003; 2012). In subaqueous fans, increase in
28
29 415 mud content improves the run-out efficiency of turbidites and increases fan size
30
31 416 (Reading and Richards, 1994). Another obvious difference is the presence of
32
33 417 dolostones in the Bolla Bolla Formation: such dolostones are absent in Pleistocene
34
35 418 TMFs. They are, however, almost ubiquitous in the Cryogenian record, typically
36
37 419 occurring immediately above the diamictite successions as cap carbonates (e.g.
38
39 420 Shields, 2005)..
40
41
42
43
44
45
46
47
48
49
50
51
52
53
54
55
56
57
58
59
60

422 The gentle regional dip of the Bolla Bollana Formation (**Fig. 5 A**) precludes
423 mapping of individual debrite megabeds, yet Quaternary analogues may allow some
424 insight into possible maximum lateral dimensions. Debrites on the Bear Island Fan are
425 elongate lobes with individual run-out distances of > 40 km (Laberg and Vorren,
426 2000; Ó Cofaigh *et al.*, 2003). They commence at ~1 km below sea level, extending

1
2
3 427 to approximately 2.5 km depth. The up-dip termination of the debrite lobes
4
5 428 approximates the palaeo-ice margin (**Fig. 9**). In addition to the generation of GDFs,
6
7 429 the accumulation of thick piles of detritus on trough-mouth fans lends them prone to
8
9
10 430 gravitational collapse (Dowdeswell *et al.*, 2002). Thus, many of the extensional faults
11
12 431 and graben structures in the NFB may represent seaward partial collapse of the fan.

13 432
14
15
16 433 Young and Gostin (1989) provided detailed descriptions and interpretations of
17
18 434 comparable successions further north, in the Yudnamutana homestead and surrounds.
19
20 435 There, a subaqueous fan system, dominated by boulder-bearing debrites with
21
22 436 subordinate turbidites, was envisaged (Young and Gostin, 1989). This interpretation is
23
24 437 fully compatible with our own and underscores that an identical range of sub-
25
26 438 environments are recognised around the Bolla Bollana outcrop belt (**Fig. 9**). It is clear
27
28 439 that the Bolla Bollana Formation contains excellent evidence for glacial sedimentary
29
30 440 processes, reinforcing the original work of Mawson (1941, 1949), and making it
31
32 441 difficult to argue for a rift-source alone as has been suggested for similar
33
34 442 Neoproterozoic diamictite successions (e.g. Eyles and Januszczak, 2004).

35
36 443
37
38
39 444 The connection between the Bolla Bollana depocentre and other sub-basins in
40
41 445 the central Flinders Ranges is obscure. Rifting is an attractive mechanism to account
42
43 446 for the different stratigraphic units preserved in the North Flinders Basin and
44
45 447 depocentres further south such as Baratta and Holowilena (Preiss, 2000). It should be
46
47 448 stressed, however, that not all sub-basins in the Flinders Ranges preserve clear
48
49 449 evidence for rifting. The Holowilena succession, for example, contains delicately
50
51 450 interbedded siltstones, diamictites, sandstones, and IRD-bearing shale (Busfield and
52
53 451 Le Heron, in review; Le Heron, 2012). Internally, that succession contains

1
2
3 452 disconformities and not angular relationships between bedsets (Le Heron, 2012)
4
5 453 which might be expected where undeformed sediments onlap rotated hangingwall
6
7 454 strata. Nonetheless, correlative successions at Oladdie Creek and Hillpara Creek, in
8
9 455 the central Flinders Ranges, reveal dramatic thickness changes along strike. These
10
11 456 testify to an irregular underlying palaeotopography, which is likely attributed to the
12
13 457 combined influence of pre- and early syn-depositional rift activity and subglacial
14
15 458 downcutting (Busfield and Le Heron, in review).
16
17
18
19 459
20
21 460

22
23 461 The Bolla Bollana Formation provides a unique window into the sedimentary
24
25 462 architecture of a trough-mouth fan (TMF). The interpretation of a TMF is doubly
26
27 463 significant. Firstly, the authors are not aware of any previously described TMFs of
28
29 464 pre-Pleistocene age, and thus the first documentation is provided herein. Secondly, the
30
31 465 Bolla Bollana is the only known outcrop example thus far described of such a fan. It
32
33 466 is probably the case that the generally large scale of these fans (O’Cofaigh, 2012) has
34
35 467 precluded their outcrop-scale interpretation in ancient strata. Whilst volumetrically
36
37 468 less significant in the fan systems than GDFs, the Bolla Bollana succession also
38
39 469 reveals the common occurrence of turbidite intervals, amplifying the importance of
40
41 470 turbidity currents in TMF models (Escutia *et al.*, 2000). The occurrence of correlative
42
43 471 turbidite and debrite-dominated successions is also well reported from subsurface
44
45 472 boreholes elsewhere in southern and central Australia (e.g. Blinman 2 borehole,
46
47 473 central Flinders Ranges; Nicholson 2 borehole, ca. 500 km NW of Arkaroola; Vines 1
48
49 474 borehole, Officer Basin) (Eyles *et al.*, 2007). A clear, glacial influence is reported
50
51 475 from those sections on account of striated and outsized clasts in laminated facies
52
53 476 (Eyles *et al.*, 2007), although it remains unclear how these underflow-dominated
54
55
56
57
58
59
60

1
2
3 477 successions relate laterally to one another. In light of our interpretations, it is possible
4
5 478 that these deposits represent an amalgam of overlapping TMFs, line-sourced detritus,
6
7 479 or somewhat more disconnected fan systems.
8
9

10 480

11 481 In the context of a Neoproterozoic snowball Earth model, Hoffman (2005)
12
13 482 argued that palaeo-ice streaming- which he inferred on the basis of irregular
14
15 483 topography within the Ghaub glacial succession of Namibia, and the occurrence of a
16
17 484 large wedge of grainstone sediment- was “not incompatible with a frozen ocean”.
18
19 485 Etienne *et al.* (2007) and Allen and Etienne (2008), meanwhile, pointed out that the
20
21 486 highly dynamic nature of tidewater ice sheets directly challenged this view. In
22
23 487 particular, the issue of resupply of snow in the accumulation zone of ablating ice
24
25 488 sheets- given the presumed arrested hydrological cycle- remains problematic.
26
27
28

29 489

30
31 490 Some 120 km to the south of Arkaroola, exceptionally exposed, age equivalent
32
33 491 successions at Holowilena, Oladdie and Hillpara Creeks, in the central Flinders
34
35 492 Ranges (Busfield and Le Heron, in review; Le Heron *et al.* 2011) reveal a highly
36
37 493 comparable stratigraphic subdivision in a series of tectonically partitioned basins.
38
39 494 These sections identify a clear non-glacial interval within the Wilyerpa Formation,
40
41 495 which yields spectacularly preserved hummocky cross strata (HCS), indicative of
42
43 496 sea-ice free conditions (Le Heron *et al.*, 2011), followed by a glacial re-advance.
44
45 497 Young and Gostin (1991) likewise identified a second major re-advance in the
46
47 498 Sturtian, represented by accumulation of the Bolla Bollana Formation. These
48
49 499 considerations suggest the Bolla Bollana Formation may correlate with the re-advance
50
51 500 succession in the central and southern Flinders Ranges and, if so, suggests deposition
52
53 501 of the TMF at Arkaroola in seas which were at least periodically unfrozen.
54
55
56
57
58
59
60

1
2
3 5024
5 503 **CONCLUSIONS**

6
7 504 The Bolla Bollana Formation is a spectacularly exposed glaciogenic succession of
8
9
10 505 Sturtian age in the Arkaroola district. This formation was first investigated by
11
12 506 Mawson (1941, 1949) but subsequently little work has been undertaken at the Tillite
13
14 507 Gorge, Stubb's Waterhole or Weetootla Gorge locations. Detailed sedimentary
15
16 508 logging at these locations, therefore, allows a detailed sedimentary model to be
17
18 509 developed as follows:

- 19
20
21 510 • Three facies associations are recognised in the Bolla Bollana Formation.
22
23 511 These are a diamictite facies association (glaciogenic debris flows with
24
25 512 subordinate ice-rafted debris), a channel belt facies association (channelized
26
27 513 turbidites with subordinate IRD) and a sheet heterolithics facies association
28
29 514 (non-channelised turbidites and subordinate IRD). A strong glacial influence
30
31 515 on sedimentation is inferred, reinforcing previous interpretations of Young and
32
33 516 Gostin (1991). A rift-related source for the diamictites is rejected.
- 34
35
36 517 • A depositional model based on detailed observations and interpretations from
37
38 518 all three facies associations proposes that the Bolla Bollana Formation was
39
40 519 deposited as a trough-mouth fan, seaward of the terminus of a small ice
41
42 520 stream. Rapid ice flux promoted high erosion rates and sediment delivery. At
43
44 521 the ice margin, GDF deposited multi-storey stacks of diamictite, many
45
46 522 deposited as megabeds. Slope failure and / or dilution of these flows
47
48 523 basinward ignited turbidites, which cut channel geometries onto the proximal
49
50 524 and medial parts of the fan. Non-channelised turbidites demonstrate well
51
52 525 organised multi-metre coarsening and fining upward motifs, interpreted to
53
54 526 record build out and abandonment of fan lobes. Laminated dolostones are an
55
56
57
58
59
60

1
2
3 527 unusual fan-lobe abandonment facies and bear superficial resemblance to post-
4
5 528 glacial “cap dolostones” elsewhere.

7 529 • Previous models of tectonic compartmentalisation a result of rifting post- 750
8
9
10 530 Ma (e.g. Preiss, 2000; Young and Gostin, 1991; Eyles and Januszczak, 2004)
11
12 531 may help in explaining dramatic regional differences in facies and internal
13
14 532 Sturtian stratigraphy. In the Bolla Bollana Formation, however, it is suggested
15
16 533 that a tectonic mechanism is not required by reference to Cenozoic trough-
17
18 534 mouth fan systems where substantive diamictite accumulations occur.

20
21 535

23 536 **ACKNOWLEDGMENTS**

25 537 The authors wish to thank Doug Sprigg for sharing with us his knowledge of the
26
27 538 pioneer’s experiences in the Arkaroola area, for permission to work in the area, and
28
29 539 general helpfulness. We are very grateful to two anonymous referees whose
30
31 540 comments significantly improved the manuscript. We also want to thank Professor
32
33 541 Nick Eyles for additional comments which helped improve the final version of the
34
35 542 paper, and Professor Stephen Rice, the handling editor, for assistance and carefully
36
37 543 considered input. This work was funded by a National Geographic Explorer Fund
38
39 544 grant to DPLeH.

42
43 545

44 546 **Figure captions**

45 547 *Figure 1:* Geological sketch map of the Arkaroola region (modified and simplified
46 548 after Coats, 1973). Note the location of the Tillite Gorge, Stubb’s Waterhole and
47 549 Weetootla Gorge sections which are shown on figure 4.

48 550

49 551

51 552 *Figure 2:* Northern Flinders Basin map, reproduced from Young and Gostin (1991).
52 553 The palaeocurrent data, shown here schematically, derive from a variety of sources
53 554 (flute casts, ripple cross laminae) and have been used to infer the development of syn-
54 555 glacial horst and graben topography (Young and Gostin, 1991). The outline of various
55 556 sub-basins are shown with a solid line, with stippling marking the internal margins of
56 557 these sub-basins.

57 558
58
59
60

1
2
3 559 *Figure 3:* Stratigraphy of the Neoproterozoic of the Arkaroola area, with subdivisions
4 560 of the Sturt glacial succession based on Young and Gostin (1989). The internal
5 561 lithostratigraphy of the Sturt glacial succession varies dramatically even over the
6 562 comparatively small region of the northern Flinders Ranges (c.f. Young and Gostin,
7 563 1988, 1989, 1990, 1991). In the Arkaroola district, a threefold division is recognised
8 564 with the Fitton Formation at the base, the Bolla Bollana Formation in the middle, and
9 565 the Lyndhurst Formation as the uppermost unit within the Yudnamutana Subgroup.
10 566 This paper specifically examines the Bolla Bollana Formation.

11 567
12 568 *Figure 4:* Detailed sedimentary logs through the Bolla Bollana Formation in the
13 569 Arkaroola district (see Fig. 1 for location of sections). Each is a partial section
14 570 through the exposure at each locality rather than a complete section. A: Stubb's
15 571 Waterhole. B: Tillite Gorge. C: Weetootla Gorge. Note that in the case of the
16 572 diamictites, the grain size in each of the logs refers to grain size of the matrix:
17 573 maximum clast size, where possible was also measured. These latter data are shown
18 574 to the right of the logs.

19 575
20 576 *Figure 5:* Representative photographs of facies within the diamictite facies
21 577 association. A: Outcrop perspective of the Tillite Gorge locality, showing thickly
22 578 bedded diamictites dipping toward the right of the photograph. B: Base of a diamictite
23 579 megabed (42-67 m, Fig. 4 B) with geologist for scale. C: Clast-poor diamictite
24 580 overlain by clast-rich diamictite, with geological hammer for scale placed at the
25 581 boundary. D: Impact structure beneath gneiss pebble in well-stratified diamictite.
26 582 Rounded clasts are quite typical. E: Undulose contact at the base of a diamictite
27 583 megabed. Note that this undulose character probably records differential compaction.
28 584 Scale bar: 1 m. F: Face of a polished and striated sandstone boulder, showing
29 585 crosscutting striation orientations.

30 586
31 587 *Figure 6:* A and B: Panoramic photo and corresponding sketch of stacked channel
32 588 geometries in the channel belt facies association. Note also the downlapping strata of
33 589 the diamictite facies association directly above. C: Low angle channel incision cutting
34 590 down towards the left of the photograph (marked by solid white line), clearly
35 591 truncating recessive siltstones, themselves infilling a channel scour. D: Low
36 592 amplitude scour at the base of a sandstone bed: evidence for erosionally-based beds
37 593 even where clear channel geometries are not observed.

38 594
39 595 *Figure 7:* A: Typical fining upward sequence, interpreted as a turbidite bed. In this
40 596 example, pebble to cobble-grade clasts beneath the hammer pass upward over 10 cm
41 597 into granular conglomerates, and finally well differentiated, moderately to well-sorted
42 598 sandstone above the hammer handle. B: Recumbent fold in a turbidite. C: Curvilinear
43 599 grooves on a sandstone surface, interpreted to record intrastratal shear in sandstones.
44 600 The absence of asperities or quartz/ calcite mineralisation discounts a tectonic origin.
45 601 D: Striated lonestone within siltstone: a putative dropstone emplaced toward the top
46 602 of a Bouma sequence. E and F: Two examples of dropstones with clear impact
47 603 structures in laminated siltstone intervals.

48 604
49 605 *Figure 8:* Representative photographs of facies within the sheet heterolithics facies
50 606 association. A: Repetitively stacked, decimetric Bouma cycles. Note coin for scale. B:
51 607 Lonestones to the left of the coin within fine-grained, climbing ripple cross-laminated
52 608 sandstone. C: Detail of photo B showing prograding crest (from right to left) of a

1
2
3 609 climbing ripple. Note that tractive velocities predicted within the field of ripple
4 610 formation (e.g. Bridge and Demicco, 2008) are insufficient to transport pebble-sized
5 611 clasts. Thus, a dropstone origin is deduced. D: Lonestone with deflected laminations
6 612 above the clast: possibly as a result of compaction. Field of view 7 cm. E: Quartzite
7 613 dropstone, with impact structure (truncation and piercing of shale laminae) beneath
8 614 the coin. Laminated dolostone (25 m, Fig. 4 C).
9 615

10 616 *Figure 9:* Simple depositional model for the Bolla Bollana Formation. We interpret a
11 617 glaciomarine basin, a general setting consistent with previous work (e.g. Coats, 1981;
12 618 Young and Gostin, 1989, 1991). Glaciogenic debris flows fed the basin, evolving into
13 619 turbidites down depositional dip. Channel belts and inter-channel areas recording
14 620 slightly finer grained turbidites are recognised. Phases of fan-lobe buildout and
15 621 abandonment are recognised, with these processes likely a result of autocyclic
16 622 switching of channel belts and sediment supply rather than basin-scale ice dynamics.
17 623 The scale of the sedimentary system, and clear evidence for a strong glacial influence
18 624 on sedimentation in all facies associations, suggests that the Bolla Bollana deposit is a
19 625 trough-mouth fan deposit, with huge volumes of glaciogenic debris supplied to a
20 626 subaqueous setting. This is the first such interpretation from the Neoproterozoic
21 627 record.
22 628
23 629
24 630

25 630 REFERENCES

- 26 631
27 632 **Allen, J.R.L.** (1984) *Sedimentary Structures: Their Character and Physical Basis*,
28 633 volumes I and II. Elsevier, Amsterdam.
29 634
30 635 **Allen, P.A. and Etienne, J.L.** (2008) Sedimentary Challenge to Snowball Earth:
31 636 *Nature Geoscience*, **1**, p. 817-825.
32 637
33 638 **Alpak, F., Barton, M.D. and Naruk, S.J.** (2013) The impact of fine-scale turbidite
34 639 channel architecture on deep-water reservoir performance. *AAPG Bulletin*, **97**, 251-
35 640 284.
36 641
37 642 **Arnaud, E.** (2012) The paleoclimatic significance of deformation structures in
38 643 Neoproterozoic successions. *Sedimentary Geology*, **243-244**, 33-56.
39 644
40 645 **Bennett, M.R.** (2003) Ice streams as the arteries of an ice sheet: their mechanics,
41 646 stability and significance. *Earth-Science Reviews*, **61**, 309–339.
42 647
43 648 **Bouma, A.H.** (1963) Sedimentary facies model of turbidites. *AAPG Bulletin*, **47** (2),
44 649 351.
45 650
46 651 **Bridge, J.S. and Demicco, R.V.** (2008) *Earth Surface Processes, Landforms and*
47 652 *Sediment Deposits*. Cambridge University Press, UK, 815p.
48 653
49 654 **Busfield, M.E. and Le Heron, D.P.** (in press) Glacitectonic deformation in the Chuos
50 655 Formation of northern Namibia: implications for Neoproterozoic ice dynamics.
51 656 *Proceedings of the Geologist's Association*. doi: /10.1016/j.pgeola.2012.10.005
52 657

- 1
2
3 658 **Busfield, M.E. and Le Heron, D.P.** (in review) Glaciodynamic signature of a Sturtian
4 659 ice sheet in the Flinders Ranges, South Australia. *Journal of Sedimentary Research*.
5 660
6 661 **Coats, R.P.** (1973) Copley, South Australia. Explanatory Notes. 1:250,000
7 662 Geological Series, Sheet SH/54-9. Geological Survey of South Australia, 38 pp.
8 663
9 664 **Coats, R.P.** (1981) Late Proterozoic (Adelaidian) tillites of the Adelaide Geosyncline,
10 665 in: Hambrey, M.J., Harland, W.B. (Eds.), *Earth's Pre-Pleistocene Glacial Record*:
11 666 Cambridge, Cambridge University Press, 537-548.
12 667
13 668 **Collinson, J.D. and Thompson, D.B.** (1987) *Sedimentary Structures*, 2nd edition.
14 669 Chapman and Hall, London.
15 670
16 671 **Corkeron, M.L.** (2007) 'Cap carbonates' and Neoproterozoic glacial successions
17 672 from the Kimberley region, north-west Australia. *Sedimentology*, **54**, 871–903.
18 673
19 674 **Daily, B., Gostin, V.A. and Nelson, C.A.** (1973) Tectonic origin for an assumed
20 675 glacial pavement of Late Proterozoic age, South Australia. *Journal of the Geological*
21 676 *Society of Australia*, **20**, 75–78.
22 677
23 678 **Dowdeswell, J.A., O'Cofaigh, C., Taylor, J., Kenyon, N.H., Mienert, J. and**
24 679 **Wilken, M.** (2002) On the architecture of high-latitude continental margins: the
25 680 influence of ice-sheet and sea-ice processes in the Polar North Atlantic. In:
26 681 Dowdeswell, J.A. & O'Cofaigh, C. (eds) *Glacier-Influenced Sedimentation on High-*
27 682 *Latitude Continental Margins*. Geological Society, London, Special Publications
28 683 203, 33-54.
29 684
30 685 **Escutia, C., Eitrem, S.L., Cooper, A.K. and Nelson, C.H.** (2000) Morphology and
31 686 acoustic character of the Antarctic Wilkes Land turbidite systems: icesheet- sourced
32 687 versus river-sourced fans. *Journal of Sedimentary Research*, **70**, 84-93.
33 688
34 689 **Etienne, J.L., Allen, P.A., Rieu, R. and Le Guerroue, E.** (2007) Neoproterozoic
35 690 glaciated basins: a critical review of the Snowball Earth hypothesis by comparison
36 691 with Phanerozoic glaciations, in: Hambrey, M.J., Christoffersen, P., Glasser, N.F.,
37 692 Hubbard, B. (Eds.), *Glacial Processes and Products*. International Association of
38 693 Sedimentologists, Special Publications, 436 pp.
39 694
40 695 **Eyles, C.H., Eyles, N. and Grey, K.** (2007) Palaeoclimate implications from deep
41 696 drilling of Neoproterozoic strata in the Officer Basin and Adelaide Rift Complex of
42 697 Australia; a marine record of wet-based glaciers. *Palaeogeography,*
43 698 *Palaeoclimatology, Palaeoecology*, **248**, 291–312.
44 699
45 700 **Eyles, N. and Januszczak, N.** (2004) 'Zipper-rift': a tectonic model for
46 701 Neoproterozoic glaciations during the breakup of Rodinia after 750 Ma. *Earth-*
47 702 *Science Reviews*, **65**, 1-73.
48 703
49 704 **Eyles, N. and Januszczak, N.** (2007) Syntectonic subaqueous mass flows of the
50 705 Neoproterozoic Otavi Group, Namibia: where is the evidence of global glaciation?
51 706 *Basin Research*, **19**, 179–198.
52 707
53
54
55
56
57
58
59
60

- 1
2
3 708 **Fairchild, I. and Kennedy, M.J.** (2007) Neoproterozoic glaciation in the Earth
4 709 System. *Journal of the Geological Society of London*, **164**, 895–921.
5 710
- 6 711 **Harrison, P. and Maltman, A.J.** (2003) Numerical modelling of reverse-density
7 712 structures in soft non-Newtonian sediments. In: van Rensbergen, P., Hillis, R.R.,
8 713 Maltman, A.J. & Morley, C.K. (eds). Subsurface sediment mobilization. *Geological*
9 714 *Society, Special Publications*, **216**, 35-50.
10 715
- 11 716 **Hart, J.K. and Roberts, D.H.** (1994) Criteria to distinguish between subglacial
12 717 glaciotectonic and glaciomarine sedimentation, I. Deformation styles and
13 718 sedimentology. *Sedimentary Geology*, **91**, 191-213.
14 719
- 15 720 **Hoffman, P.F.** (2005) 28th DeBeers Alex Du Toit Memorial Lecture, 2004. On
16 721 Cryogenian (Neoproterozoic) ice-sheet dynamics and the limitations of the glacial
17 722 sedimentary record. *South African Journal of Geology*, **108**, 557-576.
18 723
- 19 724 **Hoffman, P.F. and Schrag, D.P.** (2002) The snowball Earth hypothesis: testing the
20 725 limits of global change. *Terra Nova*, **14**, 129-155.
21 726
- 22 727 **Hoffman, P.F., Kaufman, A.J., Halverson, G.P. and Schrag, D.P.** (1998) A
23 728 Neoproterozoic Snowball Earth. *Science*, **281**, 1342-1346.
24 729
- 25 730 **Laberg, J.S. and Vorren, T.O.** (2000) Flow behaviour of the submarine glacial
26 731 debris flows on the Bear Island Trough Mouth Fan, western Barents Sea.
27 732 *Sedimentology*, **47**, 1105-1117.
28 733
- 29 734 **Le Heron, D.P.** (2012) The Cryogenian record of glaciation and deglaciation in South
30 735 Australia. *Sedimentary Geology*, **243-244**, 57-69.
31 736
- 32 737 **Le Heron, D.P., Khoukhi, Y., Paris, F., Ghienne, J.-F., Le Hérissé,** 2008. Black
33 738 shale, grey shale, fossils and glaciers: anatomy of the Upper Ordovician–Silurian
34 739 succession in the Tazzeka Massif of eastern Morocco. *Gondwana Research*, **14**,
35 740 483–496.
36 741
- 37 742 **Le Heron, D.P., Cox, G.M., Trundle, A.E. and Collins, A.** (2011) Sea-ice free
38 743 conditions during the early Cryogenian (Sturt) glaciation, South Australia. *Geology*,
39 744 **39**, 31-34.
40 745
- 41 746 **Le Heron, D.P., Busfield, M.E., Kamona, A.F.** (2013). Interglacial on snowball
42 747 Earth? Dynamic ice behaviour revealed in the Chuos Formation, Namibia.
43 748 *Sedimentology*, **60**, 411-427.
44 749
- 45 750 **Lowe, D.R.** (1982) Sediment gravity flows: II. Depositional models with special
46 751 reference to the deposits of high-density turbidity currents. *Journal of Sedimentary*
47 752 *Petrology*, **52**, 279-297.
48 753
- 49 754 **Macdonald, F.A., Schmitz, M.D., Crowley, J.L., Roots, C.F., Jones, D.S., Maloof,**
50 755 **A.C., Strauss, J.V., Cohen, P.A., Johnson, D.T. and Schrag, D.P.** (2010b)
51 756 Calibrating the Cryogenian. *Science*, **327**, 1241-1243.
52 757
53
54
55
56
57
58
59
60

- 1
2
3 758 **Maltman, A.** (1994) The Geological Deformation of Sediments. Chapman and Hall,
4 759 Cambridge. 384 pp.
5 760
- 6 761 **Marjanac, T. (1996). Deposition of megabeds (megaturbidites) and sea-level**
7 762 **change in a proximal part of the Eocene-Miocene flysch of central Dalmatia**
8 763 **(Croatia). *Geology*, 24, 543-546.**
9 764
- 10 765 **Mawson, D.** (1941) Middle Proterozoic sediments in the neighbourhood of Copley.
11 766 *Transactions of the Royal Society of South Australia*, **65**, 304–311.
12 767
- 13 768 **Mawson, D.** (1949) Sturt tillite of Mount Jacob and Mount Warren Hastings, north
14 769 Flinders Ranges. *Transactions of the Royal Society of South Australia*, **72**, 244–251.
15 770
- 16 771 **Moncrieff, A.C.M.** (1989) Classification of poorly-sorted sedimentary rocks.
17 772 *Sedimentary Geology*, **65**, 191-194.
18 773
- 19 774 **Mutti, E., Tinterri, R., Remacha, E., Mavilla, N., Angella, S. and Fava, L.** (1999)
20 775 An introduction to the analysis of ancient turbidite basins from an outcrop
21 776 perspective. *American Association of Petroleum Geologists, Continuing Education*
22 777 *Course Notes Series*, **39**. Oklahoma, USA.
23 778
- 24 779 **Ó Cofaigh, C., Taylor, J., Dowdeswell, J.A., Rosell-Melé, A., Kenyon, N.H.,**
25 780 **Evams, J. and Mienert, J.** (2002) Sediment reworking on high-latitude continental
26 781 margins and its implications for palaeoceanographic studies: insights from the
27 782 Norwegian-Greenland Sea. In: Dowdeswell, J.A. & Ó Cofaigh, C. (Eds) Glacier-
28 783 Influenced Sedimentation on High-Latitude Continental Margins. *Geological*
29 784 *Society, London, Special Publication*, **203**, 325–348.
30 785
- 31 786 **Ó Cofaigh C, Taylor J, Dowdeswell J.A. and Pudsey, C.J.** (2003) Palaeo-ice
32 787 streams, trough mouth fans and high-latitude continental slope sedimentation.
33 788 *Boreas*, **32**, 37–55.
34 789
- 35 790 **Ó Cofaigh, C., Andrews, J.T., Jennings, A.E., Dowdeswell, J.A., Hogan, K.A.,**
36 791 **Kilfeather, A.A. and Sheldon, C.** (2012) Glacimarine lithofacies, provenance and
37 792 depositional processes on a West Greenland trough-mouth fan. *Journal of*
38 793 *Quaternary Science*, DOI: 10.1002/jqs.2569.
39 794
- 40 795 **Petit, J.-P. and Laville, E.** (1987) Morphology and microstructures of hydroplastic
41 796 slickensides in sandstone. In: Jones, M.E., Preston, R.M.F. (Eds.), Deformation of
42 797 Sediments and Sedimentary Rocks. *Geological Society of London Special*
43 798 *Publication*, **29**, pp. 107–121.
44 799
- 45 800 **Preiss, W.V.** (1987) A synthesis of palaeogeographic evolution of the Adelaide
46 801 Geosyncline. In: Preiss, W.V. (Compiler), The Adelaide Geosyncline. Late
47 802 Proterozoic Stratigraphy, Sedimentation, Palaeontology and Tectonics. *Geol. Surv.*
48 803 *South Australian Bulletin*, **53**, 315–409.
49 804
- 50 805 **Preiss, W.V.** (1993) Neoproterozoic. In: Drexel, J.F., Preiss, W.V., Parker, A.J.
51 806 (Eds.), The geology of South Australia, vol. 1, The Precambrian: South Australia.
52 807 *Geological Survey, Bulletin*, **54**, pp. 170–224.
53
54
55
56
57
58
59
60

- 1
2
3 808
4 809 **Preiss, W.V.** (1999) Parachilna Sheet SH54-13. 1:250 000 scale Geological Map and
5 810 Explanatory Notes, Primary Industries and Resources South Australia. Second
6 811 edition. 52p.
7 812
8 813 **Preiss, W.V.** (2000) The Adelaide Geosyncline of South Australia and its
9 814 significance in Neoproterozoic continental reconstruction. *Precambrian Research*,
10 815 **100**, 21–63.
11 816
12 817 **Preiss, W.V., Gostin, V.A., McKirdy, D.M., Ashley, P.M., Williams, G.E. and**
13 818 **Schmidt, P.W.** (2011) The glacial succession of Sturtian age in South Australia: the
14 819 Yudnamutana Subgroup. *Geological Society, London, Memoirs*, **36**, 701-712.
15 820 doi:10.1144/M36.69
16 821
17 822 **Prélat, A., Covault, J.A., Hodgson, D.M., Fildani, A. and Flint, S.S.** (2010)
18 823 Intrinsic controls on the range of volumes, morphologies, and dimensions of
19 824 submarine lobes. *Sedimentary Geology*, **232**, 66-76.
20 825 doi:10.1016/j.sedgeo.2010.09.010.
21 826
22 827 **Reading, H.G. and Richards, M.** (1994) Turbidite systems in deep-water basin
23 828 margins classified by grain size and feeder system. *AAPG Bulletin*, **78**, 792-822.
24 829
25 830 **Rose, C.V. and Maloof, A.C.** (2010) Testing models for post-glacial ‘cap dolostone’
26 831 deposition: Nuccaleena Formation, South Australia. *Earth and Planetary Science*
27 832 *Letters*, **296**, 165–180.
28 833
29 834 **Schermerhorn, L. J. G.** (1974) Late Precambrian mixtites: glacial and/or nonglacial.
30 835 *American Journal of Science*, **274**, 673-824.
31 836
32 837 **Schermerhorn, L.J.G. and Stanton, W.I.** (1963) Tilloids in the West Congo Belt.
33 838 *Quarterly Journal of the Geological Society of London*, **119**, 201-241.
34 839
35 840 **Shanmugam, G.** (2002) Ten turbidite myths. *Earth Science Reviews*, **58**, 311-341.
36 841
37 842 **Shanmugam, G., Bloch, R.B., Mitchell, S.M., Beamish, G.W.J., Hodgkinson,**
38 843 **R.J., Damuth, J.E., Staume, T., Syvertsen, S.E. and Shields, K.E.** (1995) Basin-
39 844 floor fans in the North Sea; sequence stratigraphic models vs. sedimentary facies.
40 845 *AAPG Bulletin*, **79**, 477-512.
41 846
42 847 **Shields, G.A.** (2005) Neoproterozoic cap carbonates: a critical appraisal of existing
43 848 models and the plumeworld hypothesis. *Terra Nova*, **17**, 299-310.
44 849
45 850 **Stokes, C.R. and Clark, C.D.** (2001) Palaeo-ice streams. *Quaternary Science*
46 851 *Reviews*, **20**, 1437–1457.
47 852
48 853 **Taylor, J., Dowdeswell, J.A., Kenyon, N.H. and O’Cofaigh, C.** (2002) Late
49 854 Quaternary architecture of trough-mouth fans: debris flows and suspended
50 855 sediments on the Norwegian margin. In: Dowdeswell, J.A., O’Cofaigh, C. (Eds.),
51 856 *Glacier-Influenced Sedimentation on High-Latitude Continental Margins*. Special
52 857 Publication, vol. 203. Geological Society, London, pp. 55–71.

- 1
2
3 858
4 859 **Thomson, B.P., Coats, R.P., Mirams, R.C., Forbes, B.G., Dalgarno, C.R. and**
5 860 **Johnson, J.E.** (1964) Precambrian rock groups in the Adelaide Geosyncline: a new
6 861 subdivision. *Quarterly Geological Notes, Geological Survey of South Australia*, **9**,
7 862 1-19.
8 863
9 864
10 864 **Young, G.M. and Gostin, V.A.** (1988) Stratigraphy and Sedimentology of Sturtian
11 865 glaciogenic deposits in the western part of the North Flinders Basin, South
12 866 Australia. *Precambrian Research*, **39**, 151–170.
13 867
14 868 **Young, G.M. and Gostin, V.A.** (1989) An exceptionally thick upper Proterozoic
15 869 (Sturtian) glacial succession in the Mount Painter area, South Australia. *Geological*
16 870 *Society of America Bulletin*, **101** (6), 834–845.
17 871
18 872 **Young, G.M. and Gostin, V.A.** (1990) Sturtian glacial deposition in the vicinity of
19 873 the Yankaninna Anticline, North Flinders Basin, South Australia. *Australian*
20 874 *Journal of Earth Sciences*, **37**, 447–458.
21 875
22 876
23 876 **Young, G.M. and Gostin, V.A.** (1991) Late Proterozoic (Sturtian) succession of
24 877 the North Flinders Basin, South Australia; an example of temperate glaciation in an
25 878 active rift setting. In: Anderson, J.R., Ashley, G.M. (Eds.), *Glacial Marine*
26 879 *Sedimentation: Palaeoclimatic Significance. Geological Society of America Special*
27 880 *Paper*, **261**, 207–222.
28 881
29
30
31
32
33
34
35
36
37
38
39
40
41
42
43
44
45
46
47
48
49
50
51
52
53
54
55
56
57
58
59
60

1
2
3
4
5
6
7
8
9
10
11
12
13
14
15
16
17
18
19
20
21
22
23
24
25
26
27
28
29
30
31
32
33
34
35
36
37
38
39
40
41
42
43
44
45
46
47
48
49
50
51
52
53
54
55
56
57
58
59
60

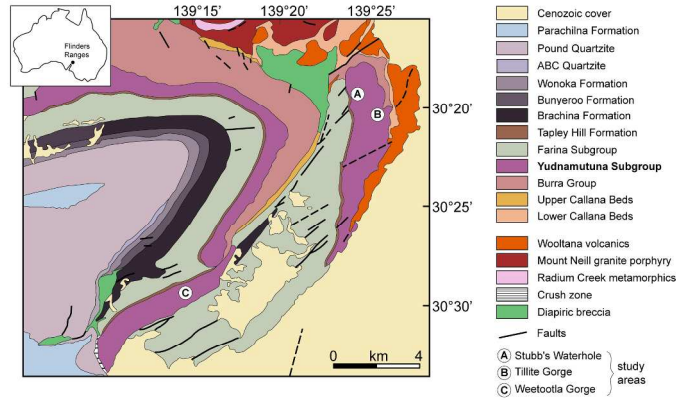


Figure 1: Geological sketch map of the Arkaroola region (modified and simplified after Coats, 1973). Note the location of the Tillite Gorge, Stubb's Waterhole and Weetootla Gorge sections which are shown on figure 4.

210x297mm (300 x 300 DPI)

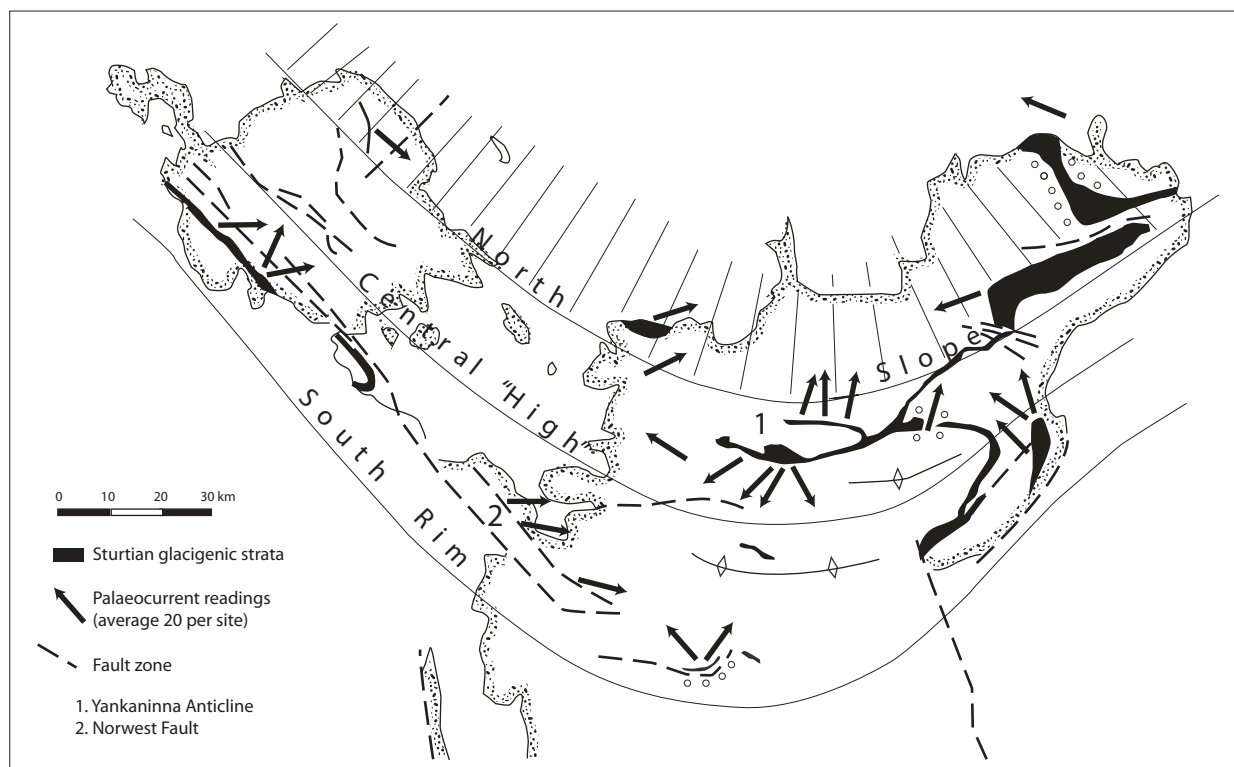


Figure 2

1
2
3
4
5
6
7
8
9
10
11
12
13
14
15
16
17
18
19
20
21
22
23
24
25
26
27
28
29
30
31
32
33
34
35
36
37
38
39
40
41
42
43
44
45
46
47
48
49
50
51
52
53
54
55
56
57
58
59
60

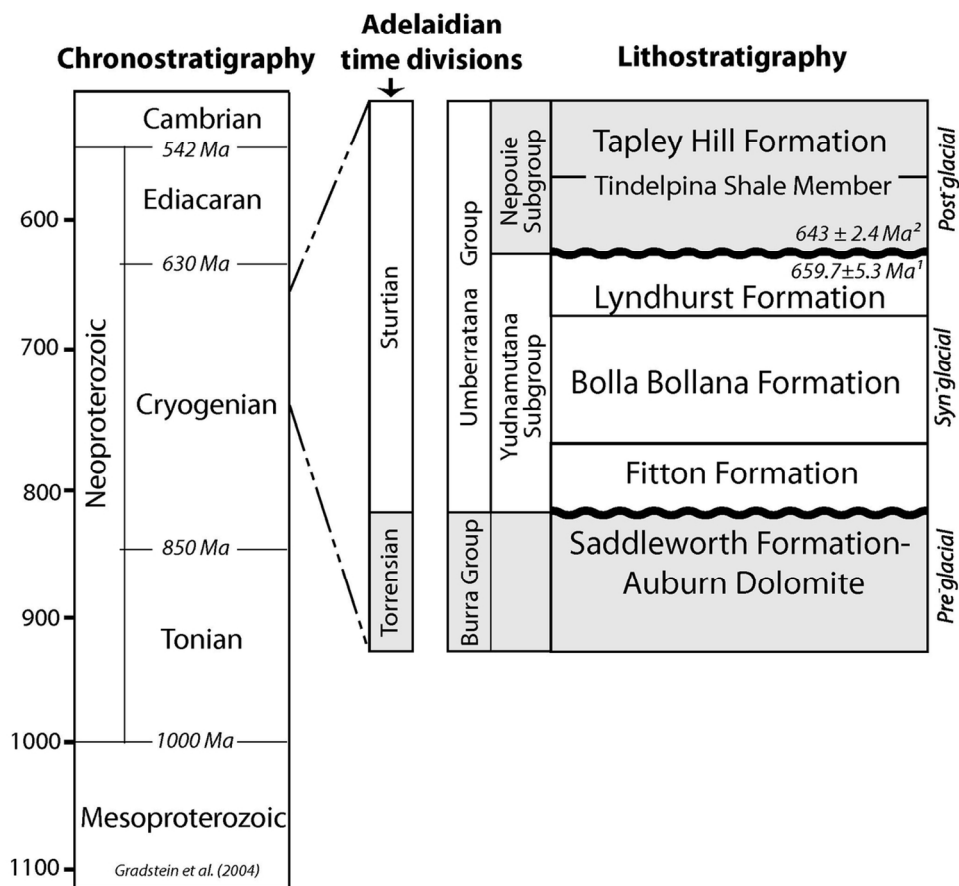


Figure 3: Stratigraphy of the Neoproterozoic of the Arkaroola area, with subdivisions of the Sturt glacial succession based on Young and Gostin (1989). The internal lithostratigraphy of the Sturt glacial succession varies dramatically even over the comparatively small region of the northern Flinders Ranges (c.f. Young and Gostin, 1988, 1989, 1990, 1991). In the Arkaroola district, a threefold division is recognised with the Fitton Formation at the base, the Bolla Bollana Formation in the middle, and the Lyndhurst Formation as the uppermost unit within the Yudnamutana Subgroup. This paper specifically examines the Bolla Bollana Formation.

108x135mm (300 x 300 DPI)

1
2
3
4
5
6
7
8
9
10
11
12
13
14
15
16
17
18
19
20
21
22
23
24
25
26
27
28
29
30
31
32
33
34
35
36
37
38
39
40
41
42
43
44
45
46
47
48
49
50
51
52
53
54
55
56
57
58
59
60

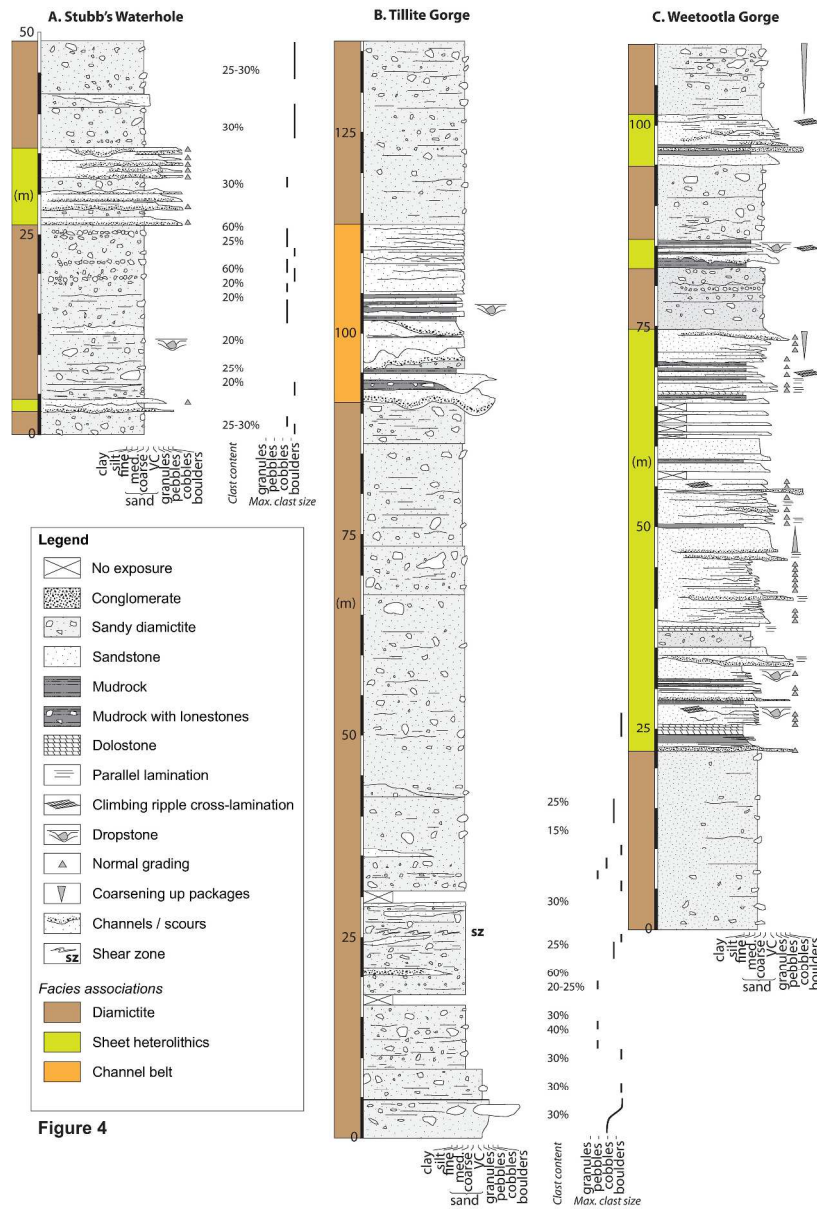


Figure 4

Figure 4: Detailed sedimentary logs through the Bolla Bollana Formation in the Arkaroola district (see Fig. 1 for location of sections). A: Stubb's Waterhole. B: Tillite Gorge. C: Weetootla Gorge. Note that in the case of the diamictites, the grain size in each of the logs refers to grain size of the matrix: maximum clast size, where possible was also measured. These latter data are shown to the right of the logs.
285x422mm (300 x 300 DPI)

1
2
3
4
5
6
7
8
9
10
11
12
13
14
15
16
17
18
19
20
21
22
23
24
25
26
27
28
29
30
31
32
33
34
35
36
37
38
39
40
41
42
43
44
45
46
47
48
49
50
51
52
53
54
55
56
57
58
59
60

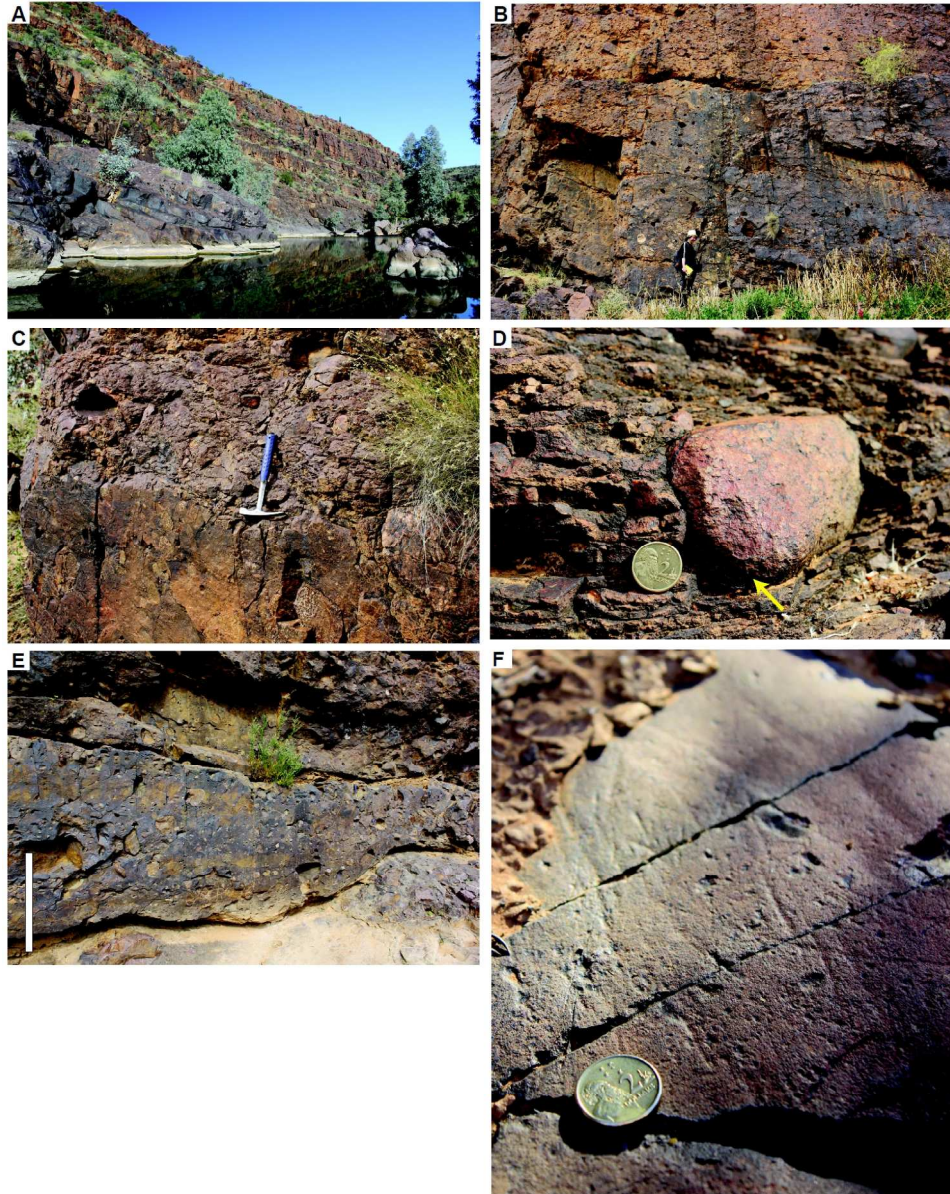


Figure 5: Representative photographs of facies within the diamictite facies association. A: Outcrop perspective of the Tillite Gorge locality, showing thickly bedded diamictites dipping toward the right of the photograph. B: Base of a diamictite megabed (42-67 m, Fig. 4 B) with geologist for scale. C: Clast-poor diamictite overlain by clast-rich diamictite, with geological hammer for scale placed at the boundary. D: Impact structure beneath gneiss pebble in well-stratified diamictite. Rounded clasts are quite typical. E: Undulose contact at the base of a diamictite megabed. Note that this undulose character likely records erosion or differential compaction. Scale bar: 1 m. F: Face of a polished and striated sandstone boulder, showing crosscutting striation orientations.

228x286mm (300 x 300 DPI)

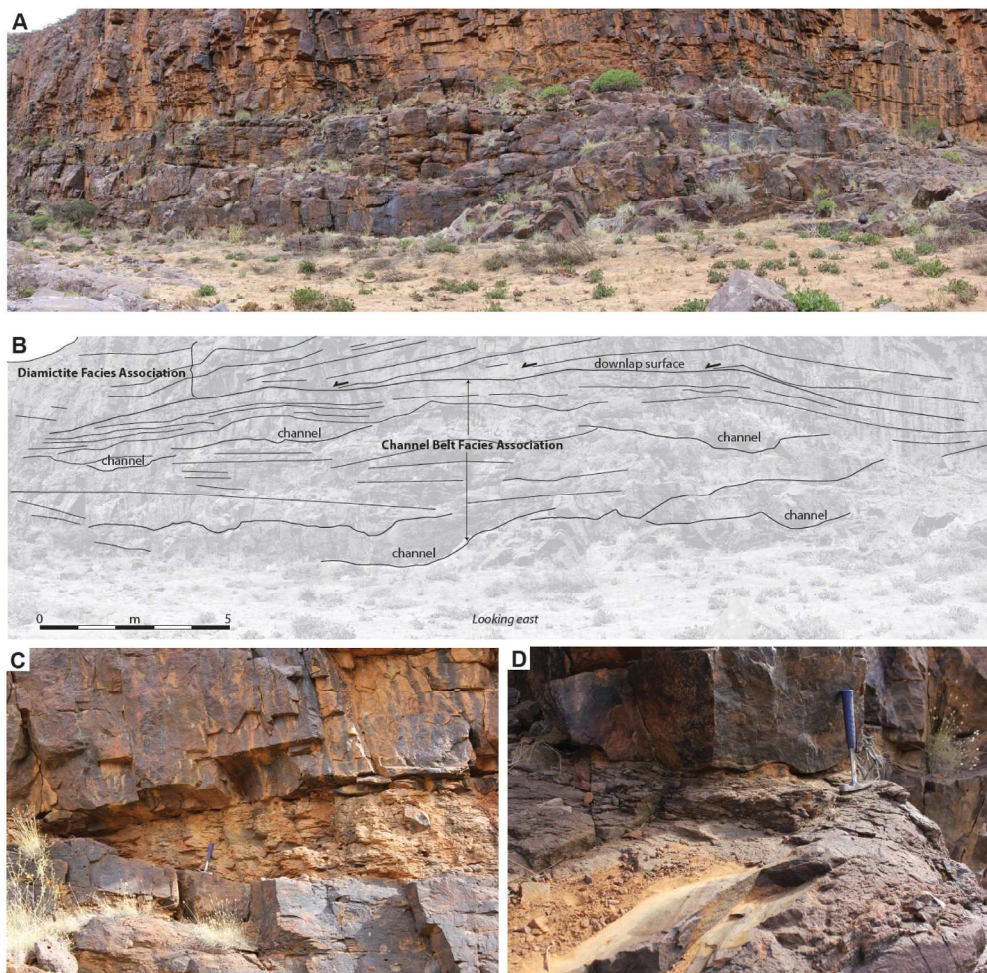


Figure 6: A and B: Panoramic photo and corresponding sketch of stacked channel geometries in the channel belt facies association. Note also the downlapping strata of the diamictite facies association directly above. C: Low angle channel incision cutting down towards the left of the photograph (marked by solid white line), clearly truncating recessive siltstones, themselves infilling a channel scour. D: Low amplitude scour at the base of a sandstone bed: evidence for erosion-based beds even where clear channel geometries are not observed.

187x182mm (300 x 300 DPI)

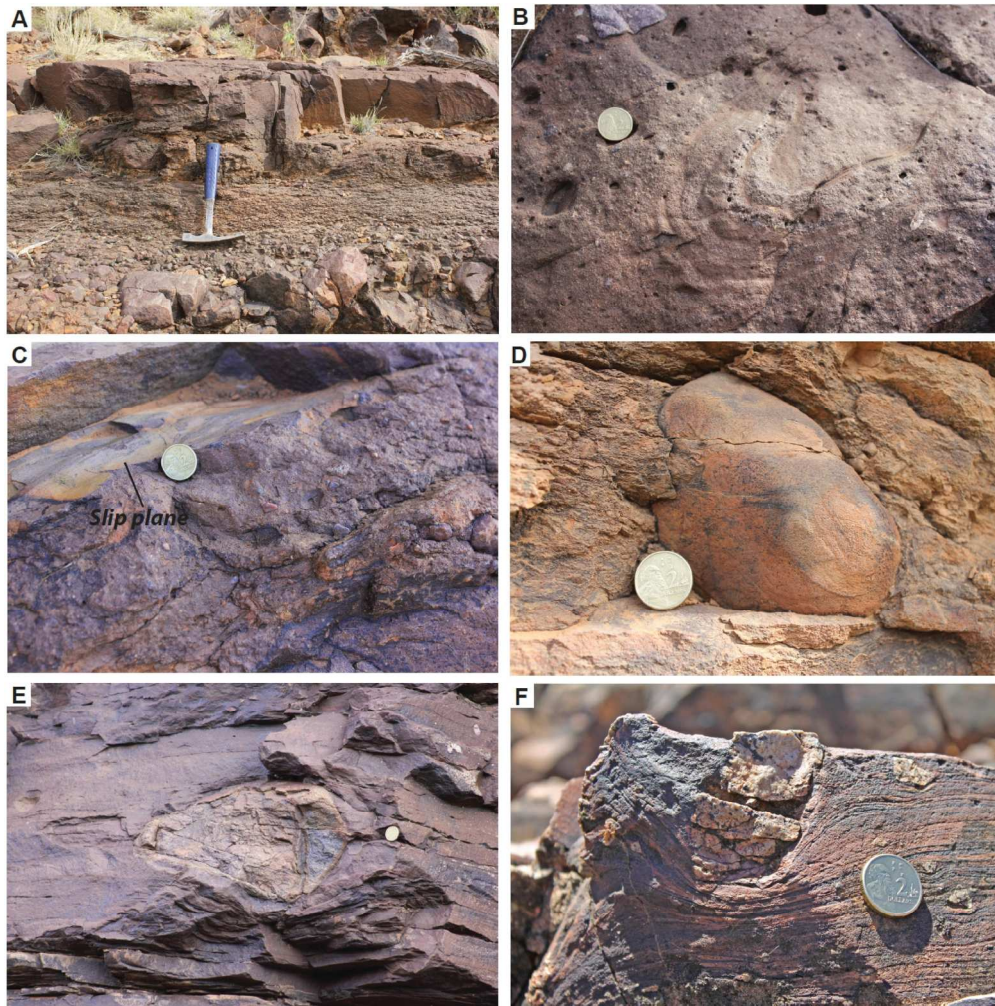


Figure 7: A: Typical fining upward sequence, interpreted as a turbidite bed. In this example, pebble to cobble-grade clasts beneath the hammer pass upward over 10 cm into granular conglomerates, and finally well differentiated, moderately to well-sorted sandstone above the hammer handle. B: Recumbent fold in a turbidite. C: Curvilinear grooves on a sandstone surface, interpreted to record intrastratal shear possibly as a result of compaction, in sandstones. The absence of asperities or quartz/ calcite mineralisation discounts a tectonic origin. D: Striated lonestone within siltstone: a putative dropstone emplaced toward the top of a Bouma sequence. E and F: Two examples of dropstones with clear impact structures in laminated siltstone intervals.

183x185mm (300 x 300 DPI)

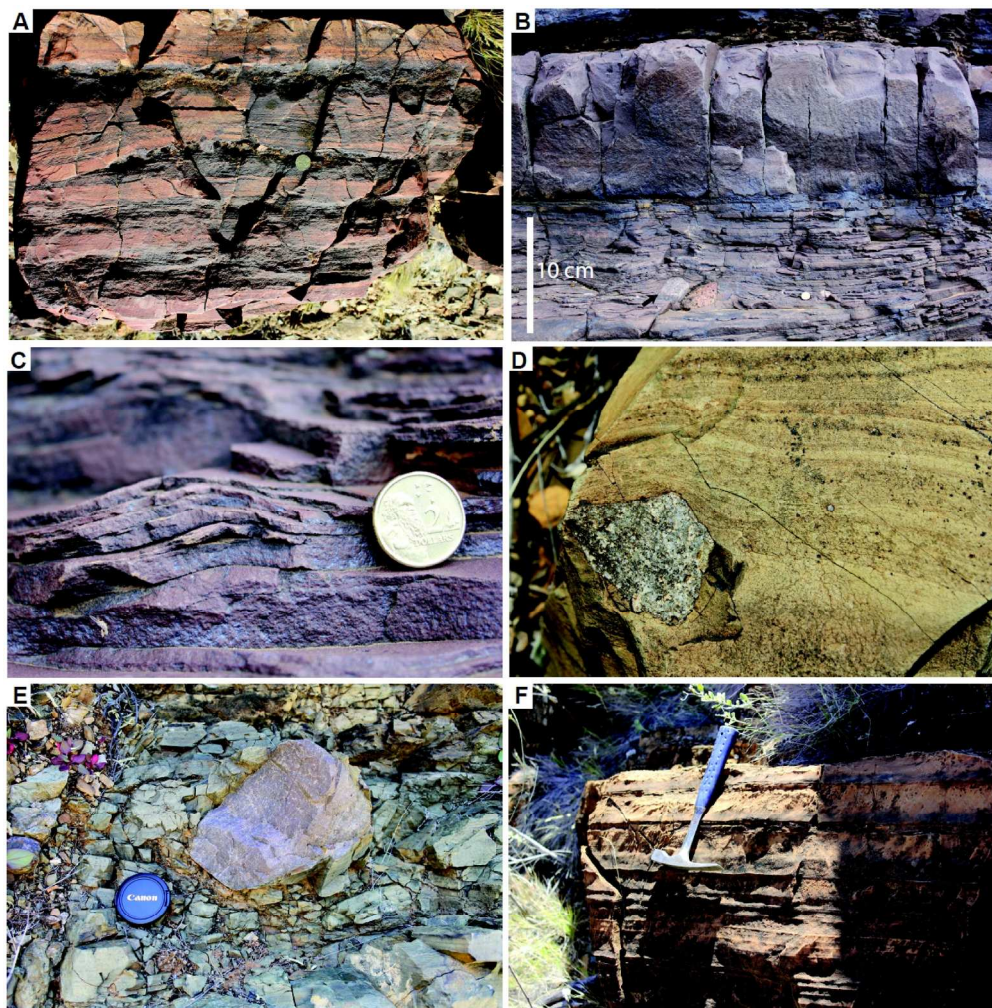


Figure 8: Representative photographs of facies within the sheet heterolithics facies association. A: Repetitively stacked, decimetric Bouma cycles. Note coin for scale. B: Lonestones to the left of the coin within fine-grained, climbing ripple cross-laminated sandstone. C: Detail of photo B showing prograding crest (from right to left) of a climbing ripple. Note that tractive velocities predicted within the field of ripple formation (e.g. Bridge and Demicco, 2008) are insufficient to transport pebble-sized clasts. Thus, a dropstone origin is deduced. D: Lonestone with deflected laminations above the clast: possibly as a result of compaction. Field of view 7 cm. E: Quartzite dropstone, with impact structure (truncation and piercing of shale laminae) beneath the coin. Laminated dolostone (25 m, Fig. 4 C).

197x198mm (300 x 300 DPI)

1
2
3
4
5
6
7
8
9
10
11
12
13
14
15
16
17
18
19
20
21
22
23
24
25
26
27
28
29
30
31
32
33
34
35
36
37
38
39
40
41
42
43
44
45
46
47
48
49
50
51
52
53
54
55
56
57
58
59
60

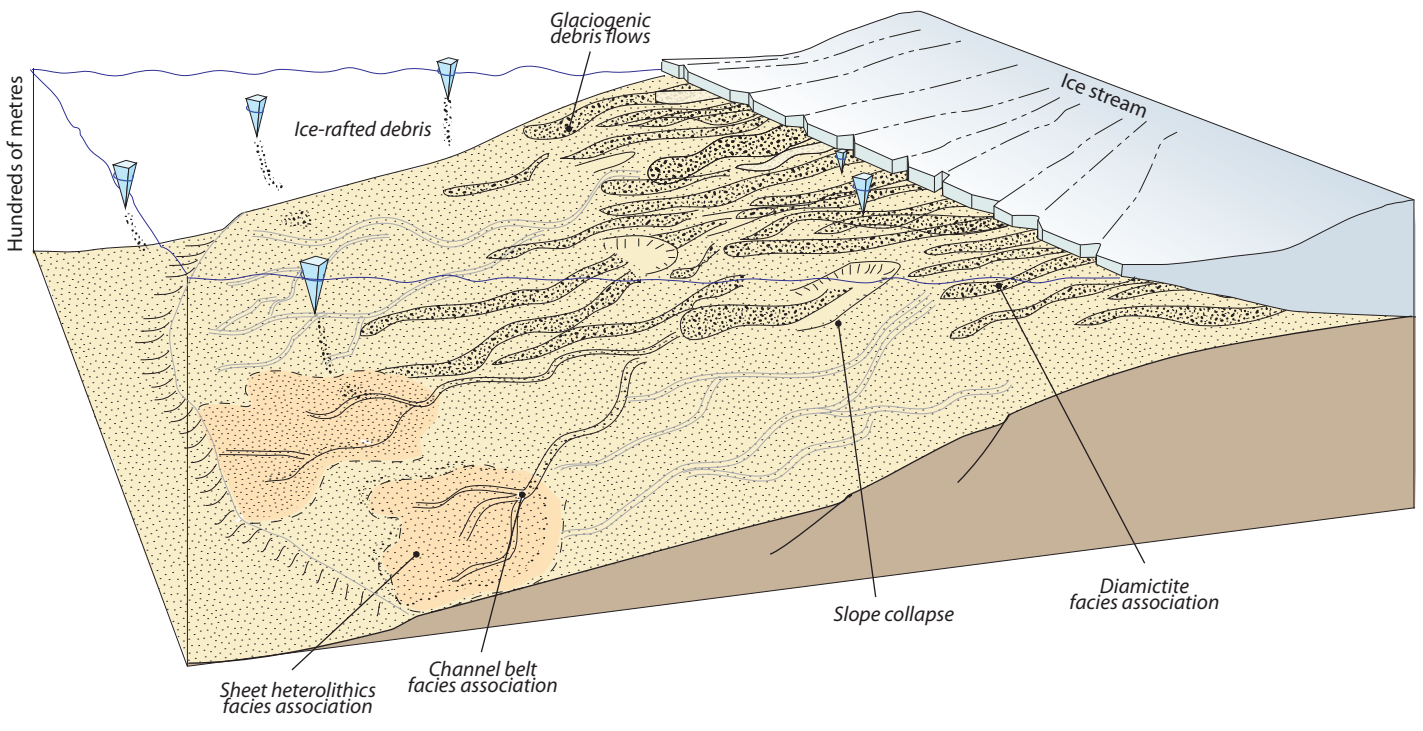


Figure 9